電気学会論文誌●（●●●●●●●部門誌）
IEEJ Transactions on ●●●●●●●●●●●●●●●●
Vol.●● No.● pp.●-●● DOI: ●.●●/ieejeiss.●●.●

Paper

High-Efficiency Charge/Discharge Control of Hybrid Energy Storage System Based on High-Efficiency Voltage Range

Elosegui Garcia Pablo* Non-member, Hitoshi Haga*a) Member

In order to reduce the fluctuation in the power grid due to the power generated by renewable energy sources, a grid connected hybrid energy storage system, which combines lithium-ion batteries and ultra-capacitors is used. In this paper, a new high-efficiency charge/discharge control method for power division as well as stored energy balance is proposed. The battery bank, ultra-capacitor bank, and power converters are individually analyzed. The control method is based on the high efficiency voltage range (HEVR), which is a new method of determining the highest efficiency work-point of the energy storage systems. A 1 kW scaled prototype is used to assess the performance of the proposed system. The experimental results show that the proposed system achieves a higher total efficiency than the conventional method, while being able to control the energy balance of the storage devices.

Keywords : renewable energy, energy storage, high efficiency, battery, ultra-capacitor, storage control

1. Introduction

The increasingly rising usage of high powered renewable energy production has an inherent issue in its nature. Due to the ever-changing climatological conditions, the power output of these installations varies significantly, which makes the grid power flow fluctuate [(1)-(4)]. In order to compensate this fluctuation, energy storage systems such as batteries and ultra-capacitors have been used to absorb or deliver the remaining energy. These solutions integrate a high powered energy storage component such as ultra-capacitors, and a high energy storage component such as lead or lithium batteries, each with a power conversion phase for connecting them to the grid. Different power division methods have been used for defining the power delivery of both branches (battery and ultra-capacitor). In [(5)] FDAM is used for dividing the power reference based on frequency, the high frequency component being supplied by the EDLC and the low component by the battery. In [(6)] ADAM is used, where the battery supplies power up to a limit and the EDLC supplies the rest. However, none of these take the energy storage balancing into account, nor the internal behavior of the energy storage devices.

This paper proposes a high-efficiency energy storage balancing and power delivery control method, based on the high-efficiency voltage range (HEVR) of both the batteries and ultra-capacitors (EDLCs). The proposed system combines Li-ion batteries in one branch, and EDLCs (electrolytic double layer capacitors) which can individually be controlled. The control method uses previously determined HEVRs, which is the voltage range of the energy storage system where the efficiency is the maximum, in order to maintain the highest efficiency possible, as well as controlling the storage device´s energy balance. Using this method, three different modes are automatically selected, which decide the instantaneous power division. The power delivery of the battery and EDLC branch are separately determined based on the power reference as well as SOC state of the storage devices, opposed to the conventional methods, which only take the power reference in to account.

The experimental results show that the proposed control method is able to supply and absorb the excess energy of the grid while having a higher efficiency than the conventional methods. Moreover, due to the nature of the HEVRs, the energy balance of the storage devices is control in an active manner, which the conventional methods did not provide.

2. Principles of the stabilization power delivery

The system is composed by a grid connected AC/DC, where the DC side is divided in two branches. The first branch has a DC/DC converter and a battery bank, while the second branch has another DC/DC and an EDLC bank. These two branches are used separately, the battery bank is usually used for its high energy storage capabilities, whereas the EDLCs are used due to their high discharge currents and fast response. Fig. 1 shows this configuration.

In order to determine the power delivery for both branches, two main conventional methods have been used: FDAM (frequency division allotment), where the reference power is divided by the frequency of its components; and ADAM (amplitude division allotment) where the reference power is divided by the amplitude.

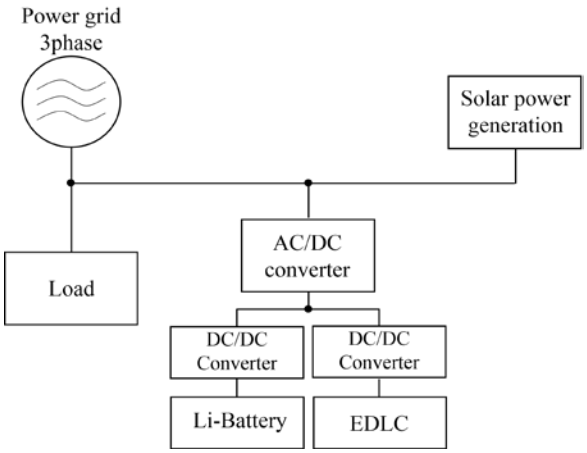

Fig. 1. Configuration of the grid connected system.

a) Correspondence to: Hitoshi Haga.
e-mail: hagah@vos. nagaokaut.ac.jp
*Nagaoka University of Technology
1603-1, Kamitomioka-cho, Nagaoka-city, Niigata, Japan 940-2188

Fig. 2 shows the principles of the conventional methods [5]-[6]. The power reference in Fig. 2 (b) demonstrate the FDAM method, where the power division is determined by a simple low pass filter. Fig. 2 (c) shows the ADAM method, where the power division is determined by a simple maximum limiter. These two methods have only one input, which is the reference power. In order to understand the theoretical background of the proposed method, first the power loss and HEVR analysis will be explained.

3. High-Efficiency Voltage Range (HEVR)

The HEVR method developed in this paper follows the next line of thought: Both the battery side and the EDLC side of the system have an energy storage device and a converter connected. These have characteristic power losses, and can be controlled independently. On the one hand, the battery´s losses are related to the equivalent series resistance (ESR), while the converter has it´s switching and conducting losses. On the other hand, the EDLC´s losses are related to the ESR as well as to the self-discharge phenomenon, plus the converter losses. In this chapter, all of this losses are experimentally quantified, in order to create a simulation model of the system, and determine the HEVR of both the battery side and the EDLC side.

3.1 Battery losses

As previously said, the battery losses are related to the ESR [7]-[8].

$$P_{loss} = I^2 ESR \quad \cdots\cdots (1)$$

In order to calculate the power loss, first the ESR needs to be estimated. The ESR depends mostly on the instantaneous current, SOC and temperature of the battery [9]. The battery pack used for the ESR experiment is a 12 series of 31 Ah 3.6 V Li-ion, which combined have a maximum 50 V. A thermostatic chamber is used to control the battery´s temperature at 20 ºC, as the final experiments will able carried out at room temperature, and a series of experiments are carried out at 0.01 C to 0.36 C and at 90% to 10% SOC. The battery is discharged at different current rates, and the voltage drop of the battery is measured at every 10% SOC discharge [10]. The resulting voltage drop is divided by the instantaneous current and the ESR for each case is obtained. This data is arranged using Matlab, in a four three dimensional graph (Fig. 3). The data points are interpolated in order to have more accuracy. The ESR does not suffer a noticeable change either with the C rate or the Depth of Discharge (DOD). The ESR value has a maximum of 30 mΩ and a minimum of 27 mΩ. This data is used for the battery model in the simulation which will later be explained.

3.2 EDLC losses

The power losses of the EDLC´s depend on the ESR and also on the self-discharge of the cell [11]-[12]. First, the same experimental tests as with the battery pack were carried out. In this case, the EDLC pack is formed by 63 2400 F 2.5 V EDLCs, arranged in 21S3P, which combined have 2.5 Ah and a maximum of 52.5 V. The tests were carried out at 20 ºC, 100% to 20% SOC and 0.1 C to 10 C. The ESR does not seem to change with SOC or current, just a 2%, which is inside the margin of error. The ESR ranges from 1.38 mΩ to 1.42 mΩ, which is about 30 times lower than in the case of the battery pack. Besides the ESR, the self-discharge also contributes to the power loss of the device, due to the imperfections in the EDLC layers, which create a parallel resistance [13]-[14]. In order to quantify this power loss, the EDLC pack was charged to 100% of its capacity at 2 C, and its voltage was measured for 4 hours.

Fig. 5 shows the decline in stored energy due to the self-discharge. The EDLC pack tested loses the 30% of its charge in just an hour

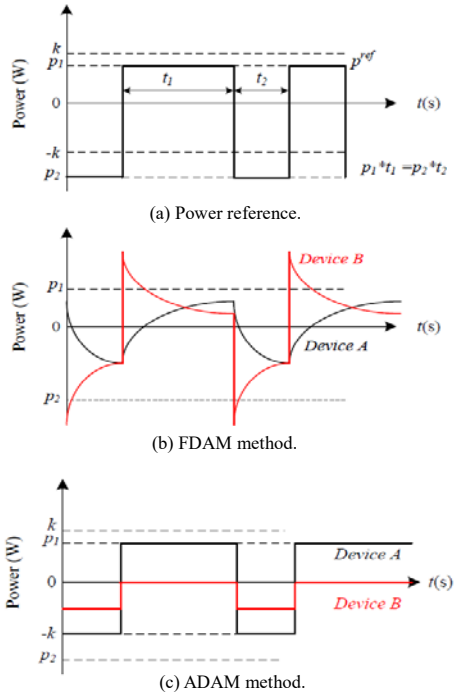

Fig. 2 Conventional methods of power division example.

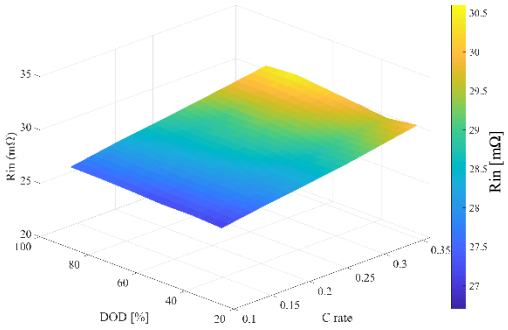

Fig. 3. Battery ESR relation with C rate and DOD.

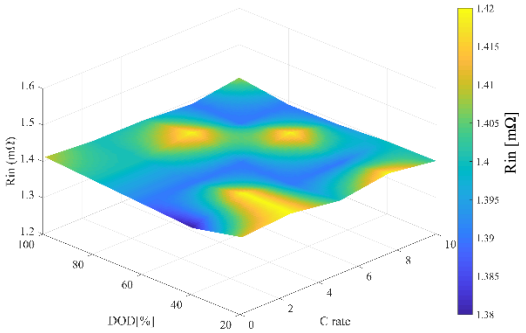

Fig. 4. EDLC ESR relation with C rate and DOD.

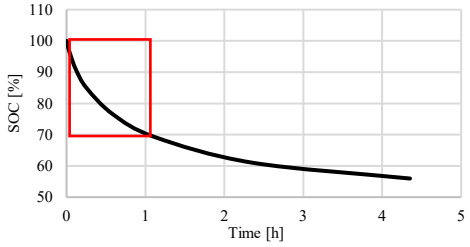

Fig. 5. EDLC self-discharge trend in a 4-hour period.

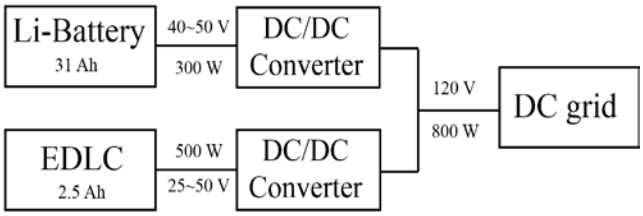

Fig. 6. Fluctuation balancing system schematic.

(highlighted with the red square), which means that even if the EDLC pack is not being used, there are power losses. The power loss decreases as the SOC of the device decreases, suggesting that using the device at a lower SOC will increase its efficiency.

Both the data of the ESR, as well as the self-discharge data are used for creating the EDLC pack model in simulation.

3.3 Converter losses

Fig.6 shows the experimental setup for obtaining the converter loss characteristics. The converter losses can easily be calculated by using equations, but in order to the data to be as close to reality as possible, an experimental setup was built.

As already mentioned, the battery pack and the EDLC pack have a maximum voltage of 50 V, 300 W maximum power for the battery and 500 W for the EDLC. The grid is a DC supply/load, as the DC/AC converter´s efficiency does not change depending on the control strategy, the power reference in it will always be the same regardless of the control method. This grid is at a constant 120 V. Due to this, the converters need to work as step-down when the energy flows into the energy storage, and as step-up when energy has to be provided to the grid.

With this information, two buck-boost converters were built, with a maximum power output of 300 W and 500 W respectively. In order to quantify the efficiency of the converters, tests from 50 W to 800 W were carried out, the power difference at the input and the output of the converter measured and the efficiency was obtained. The experiment shows that the converters are more efficient at higher voltages, there is a clear increase in power loss when the battery of EDLC side voltage decreases. This data is used in order to create the converter model in the simulation for the HEVR calculation, as well as for the control method simulation.

4. HEVR simulation

The first thing for building the control method is determining the HEVR of both the battery side and the EDLC side. Using the data from the experiments, models for the battery pack, EDLC pack and converters are created in Matlab and PSIM. This models can be simulated in order to know the HEVR. The PSIM simulation inputs real PV generation data and different control methods can be tested for the fluctuation balancing. This simulation works with the Matlab models previously shown. The simulation can be used to determine the HEVR, setting the battery and EDLC packs to a range of SOCs, the total efficiency of the energy storage, combined with the converter´s efficiency is obtained.

The battery side´s efficiency is higher when the voltage of the device is high. This supports the prediction made when testing the battery. The battery´s ESR does not change much with the voltage, but the lower the voltage, the higher the current for the same power reference. This increases the power losses of the battery, and as shown in Fig. 8, the efficiency of the converter decreases with the voltage. Thus, it is possible to determine the HEVR of the battery to be the upper half of the graph, 46 V to 50 V. The efficiency decreases as power increases, this is why the battery is limited to 300 W, which is also the rated power of the DC/DC converter.

As regards the EDLC side, the opposite effect can be seen. The lower the voltage the higher the efficiency. This happens due to the self-discharge of the EDLC.

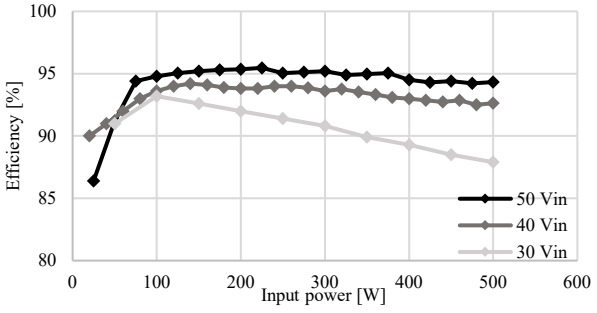

(a) Boost mode efficiency at 30, 40 and 50 Vin, 120 V output.

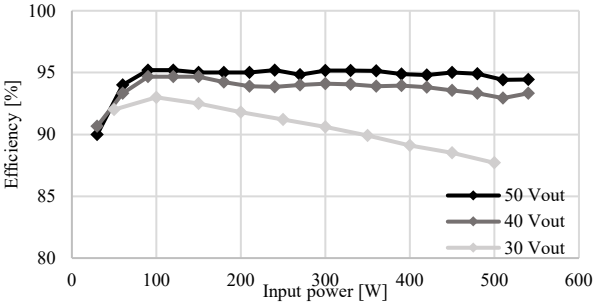

(a) Buck mode efficiency at 30, 40 and 50 Vout, 120 V input.

Fig. 7. Double buck-boost converters efficiency trend with input power.

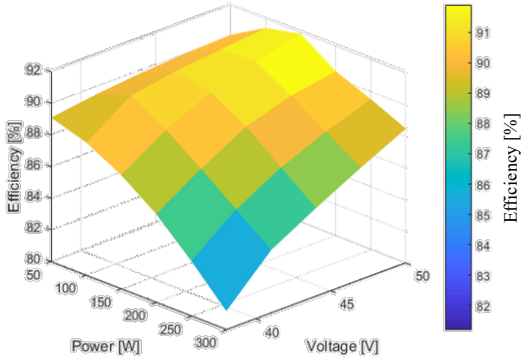

(a) Battery pack and battery side converter combined efficiency at 38 V to 50 V (10% SOC to 95% SOC).

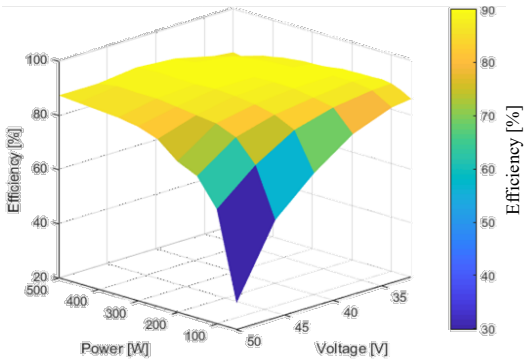

(b) EDLC pack and EDLC side converter combined efficiency at 33 V to 50 V (39% SOC to 95% SOC).

Fig. 8. Combined efficiency of battery side and EDLC side.

Fig. 5 shows that the self-discharge is stronger at higher voltages. This effect is so strong that, although the converter has a lower efficiency at low voltages, the converter losses are shadowed by it. The EDLC pack was not tested at a lower voltage than 30 V due to the fact that the current would be too high for the designed converter. The efficiency decreasing at low power just shows that if the EDLC is not used much, the self-discharge loss is predominant. Thus, it is possible to determine that the HEVR of the EDLC side is around 35 V to 40 V, as it avoids the rapidly decreasing area of the graph. While having more than 75% efficiency.

5. Proposed power division method

The proposed method takes into account the power reference, as well as both the battery and EDLC banks´ voltage. This allows for a more precise, technology specific control method.

Fig. 9. Shows the different modes that the proposed method Active Threshold Balancing Method (ATBM) works at. These modes are selected depending on the power reference and battery and EDLC voltages according to Fig. 13. The modes follow the voltage threshold laws displayed in Fig. 4, according to the HEVR.

In the synchronous mode, 67% of the power is provided/absorbed by the battery, while the remaining 33% is provided/absorbed by the EDLC pack. This ratio was decided experimentally, as it is the highest efficient ratio which can supply power for the 2.5-hour experiment, as shown in Table 1. However, depending on the parameters of the system, this ratio can be modified in order to obtain the highest efficiency for a determined working time. This allows for a higher efficiency than using only one of the technologies at a time. Although the equivalent series resistance of the batteries is higher than the EDLC´s, as the battery packs are less costly, typical applications have a higher battery energy capacity than EDLC, therefore improving the energy stability of the system.

In the overpower mode, when the power reference exceeds the power limit of the battery, the battery is set to the power limit, while the EDLC pack provides/absorbs the rest. This is due to the high power rating of EDLCs, compared to the Lithium batteries.

In the capacitor recovery mode, if the EDLC voltage goes below the minimum voltage threshold (Fig. 10), as soon as the power reference changes to positive (towards the energy storage) the EDLC pack absorbs the 67% of the power, while the 33% is absorbed by the battery pack. The low energy EDLC pack is therefore charged twice as fast and pulled back inside the HEVR.

6. Experimental analysis

6.1 Experiment structure and system response

In order to verify the performance obtained through simulations, a 1 kW experimental prototype was built. Fig.11 shows the experimental system and Fig.12 shows the control block diagram of the proposed method. In this paper, a DC grid is configured to apply PV power fluctuations to the DC bus. The solar power generation is simulated by programmable power supply and electronic load. The battery power reference (P_{bat}^*) is divided by the actual voltage of the LiB battery (V_{bat}) so that the current reference i_1^* is created. The same is done with the EDLC (P_{cap}^*) to create the current reference i_2^*. P_{bra}^* is the compensation power reference, which is obtained by the grid-power and rate of change limiter (limit value is set to 10W/s). Fig.14 shows the power fluctuation experimental prototype front view.

The setup is comprised of the same elements as shown in Table 2. In addition to the battery pack, EDLC pack and DC/DC converters, a TMS320x28069 is used in order to control the whole

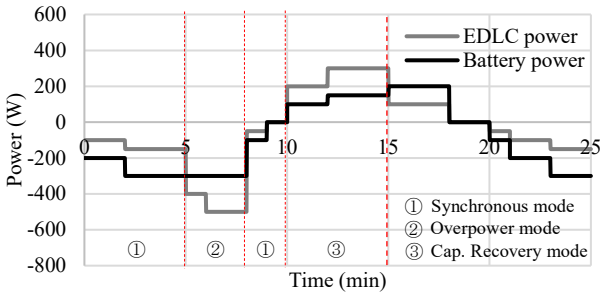

Fig. 9. Proposed method ATBM (Active Threshold Balancing Method) example power division example.

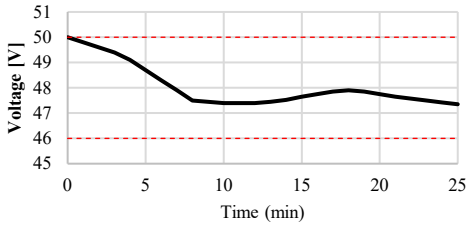

(a) Battery voltage and threshold of the example.

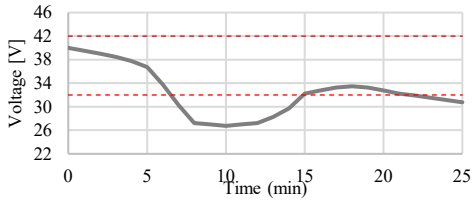

(b) EDLC voltage and threshold of the example.

Fig. 10 Battery and EDLC pack voltage trends and HEVR thresholds.

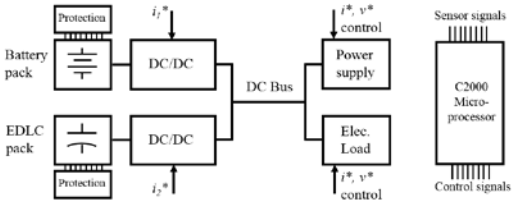

Fig. 11. Experimental system configuration

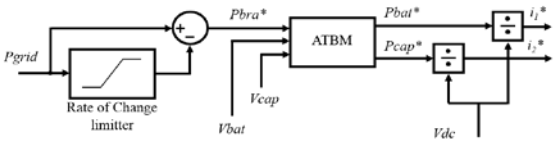

Fig. 12. Experimental proposed control block diagram

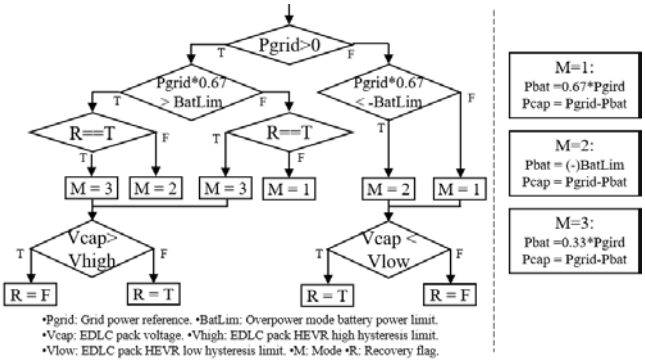

Fig. 13. ATBM flowchart

Table 1: ATBM power ratio experiments

Ratio	**25%**	**33%**	**50%**
Total Efficiency [%]	82.6	85.2	86.6
Working time test	Passed	Passed	Failed

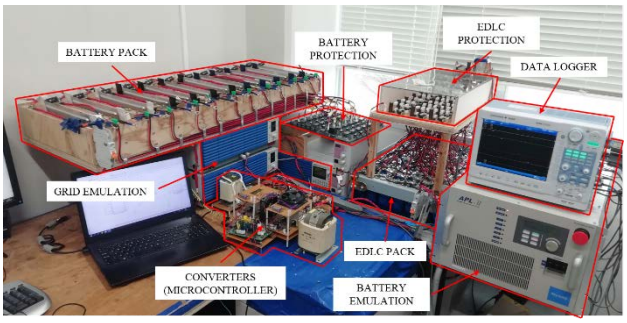

Fig. 14. Power fluctuation experimental prototype front view

Table 2. Experiment component specifications

Component	Voltage	Power	Capacity
Battery Pack	38 V to 50 V	300 W	31 Ah
EDLC pack	25 V to 50 V	500 W	2.5 Ah
Battery converter	38 V to 50 Vin 120 Vout	300 W	
EDLC converter	25 V to 50 Vin 120 Vout	500 W	
Grid	120 V	1000 W	

system. TheTMS320x28069 is programmed using Simulink. This program runs in real time, where the input is real irradiation data. This data has been obtained using photosensitive sensors in order to calculate the sun irradiation of an average Japanese summer day. Both of the experiments start with 47 V on the battery pack and 46 V on the EDLC pack. The first experiment was done using the ATBM algorithm (Fig13). First the grid power reference is examined; if it is negative (discharging), it is multiplied with the ration of the battery (0.67) is order to see if the battery would exceed its maximum power limit. If this is true, the overpower mode is selected (M = 2), if not, the synchronous mode is selected (M = 1). After this, as the EDLC was discharging, its voltage is compared with the low hysteresis point of the HEVR, if it is lower, the flag for recovery mode is activated (R = T), if not, it is not activated (R = F). Regarding the case of charging, once again the grid reference times the ratio is compared with the battery´s power limit. If true and the recovery flag is on, Recovery Mode is chosen (M = 3), if not, Overpower mode is chosen. If the battery´s power reference is lower than its power limit, once again the recovery flag is evaluated in order to choose the Recovery mode or the synchronous mode. As the EDLC was charging, its voltage is compared with the high HEVR hysteresis voltage in order to activate or deactivate the recovery flag.

Next, the performance of the system was tested using the ADAM method. And finally the FDAM method. The sun radiation input data spans two and a half hours.

Fig. 15 shows the grid power reference. This reference is obtained from the sun irradiation data, which is filtered using a Rate of Change algorithm in order to determine how much power needs to be supplied to or be absorbed from the grid [5].

The resulting battery and EDLC power reference are as expected. The battery supplies most of the power when the voltages are inside the HEVR thresholds. When the battery power reference exceeds the 300 W limit, the control changes to overpower mode, where the EDLC pack supplies the rest of the power. This power limit is show with a red line on Fig. 16.

2400 seconds into the experiment, the voltage of the EDLC pack goes below the minimum HEVR threshold (35 V), thus the system changes to recovery mode as soon as the power reference changes to positive (charging). In this experiment, the maximum HEVR threshold has not been implemented. The period being on recovery mode is expressed with a red square in Fig. 17 and Fig. 18. This period ends when the voltage reaches a hysteresis maximum, this time located at 40 V. The correct implementation of the recovery mode is thus verified, with the EDLC absorbing two thirds of the power reference, while the battery absorbs one third.

Regarding the ADAM tests, shown in Fig. 19 and Fig. 20, which have the same grid reference data as the in the ATBM experiment, the results show that most of the power is supplied using the battery, whereas the EDLC only works at power peaks over 300 W. This 300 W limit is the same as in the ATBM method for the sake of fair comparison.

Finally, the FDAM method was tested. As it is based on a low pass filter (cutoff 20 sec.), the battery´s output is smooth whereas the EDLC ´s output is overall very aggressive, with many sudden power increases and decreases. A very significant matter to notice is the effect of the low pass filters phase delay. It is shown in Fig. 21 and Fig. 22 that when the grid power reference has a sudden change, the EDLC has to compensate the slow response of the battery. This results in power flowing from the battery to the EDLC and vice versa, which creates additional power loss. Thus, the actual power conversion when using the FDAM will always be bigger than the required for grid stabilization.

The experimental results show that the proposed system is able to apply the ATBM control method. The control method behaves as theoretically planned and the three modes are shown to be applied successfully. The ATBM uses more the EDLC pack than the ADAM does, which in theory should decrease the power losses. In order to objectively compare the performance of the three methods, efficiency analysis is needed.

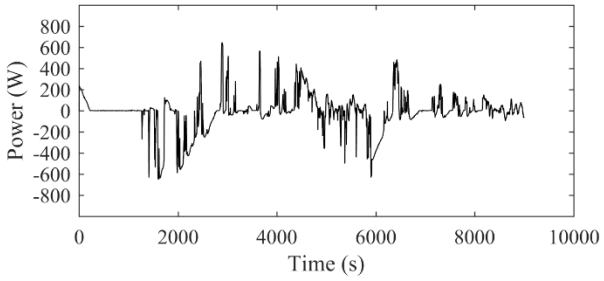

Fig. 15. ATBM experiment grid power reference.

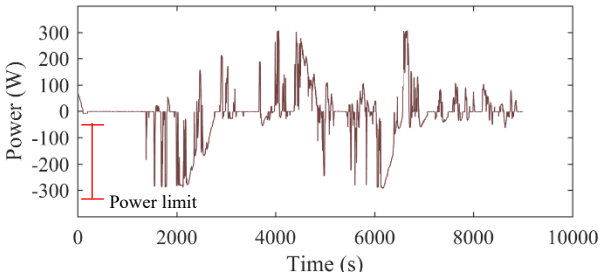

Fig. 16. ATBM experiment battery pack power reference after applying ATBM division method.

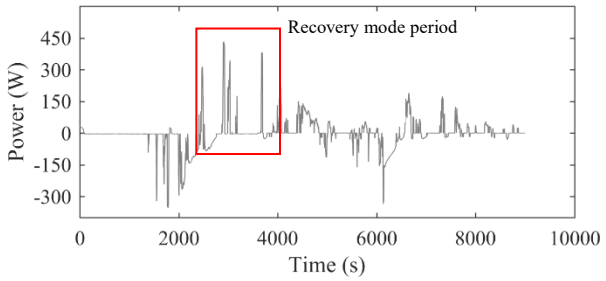

Fig. 17. ATBM experiment EDLC pack power reference after applying ATBM division method.

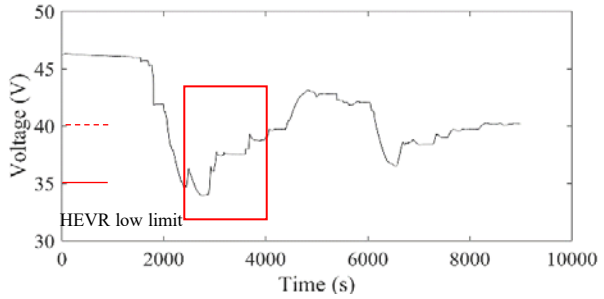

Fig. 18. ATBM experiment EDLC pack voltage response with recovery mode effect and threshold.

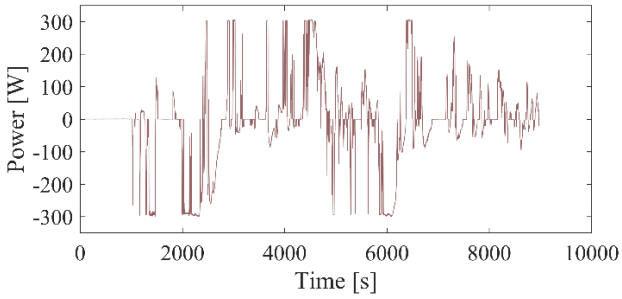

Fig. 19. ADAM experiment battery pack power reference after applying ADAM division method.

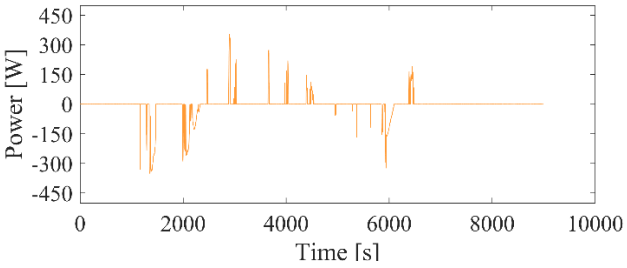

Fig. 20. ADAM experiment EDLC pack power reference after applying ADAM division method.

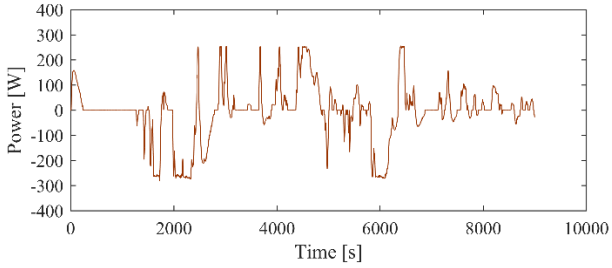

Fig. 21. FDAM experiment battery pack power reference after applying FDAM division method.

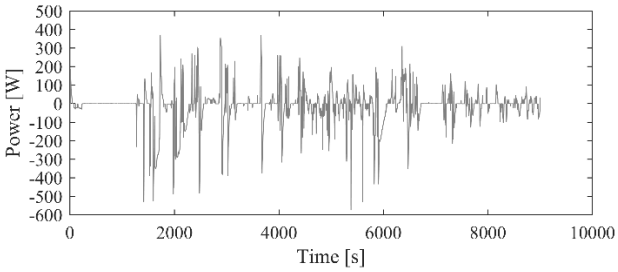

Fig. 22. FDAM experiment EDLC pack power reference after applying FDAM division method.

6.2 Efficiency analysis criteria

The efficiency calculation of the different parts (Battery pack, EDLC pack, converters) differs depending on the direction of the energy transfer. In other words, two different formulas are used for each part, one for charging and one for discharging.

For charging:

$$\eta_{bat} = \frac{\int I_b V_b - \int {I_b}^2 \, ESR}{\int I_b V_b} \quad \cdots\cdots (2)$$

$$\eta_{DCDC} = \frac{\int I_l V_l}{\int I_h V_h} \quad \cdots\cdots (3)$$

$$\eta_{EDLC} = \frac{C\left({V_2}^2 - {V_1}^2\right)p}{2s\int I_c V_c} \quad \cdots\cdots (4)$$

For discharging:

$$\eta_{DCDC} = \frac{\int I_h V_h}{\int I_l V_l} \quad \cdots\cdots (5)$$

$$\eta_{bat} = \frac{\int I_b V_b}{\int I_b V_b + \int {I_b}^2 \, ESR} \quad \cdots\cdots (6)$$

$$\eta_{EDLC} = \frac{2s\int I_c V_c}{C\left({V_2}^2 - {V_1}^2\right)p} \quad \cdots\cdots (7)$$

where I_l is the current of the low side of the DC converter, V_l is the low side voltage, I_h and V_h are the high side current and voltage, C is the capacitance of an individual EDLC cell, I_c and V_c are the EDLC pack´s current and voltage, p is the number of EDLC cells in parallel, s the number of series cells, and V_1 and V_2 the voltage of the EDLC pack at the beginning and the end of the charging or discharging period.

6.3 Final performance comparison

After applying equations (3) to (7) to the experimental results, the efficiency of the FDAM, ADAM and ATBM is calculated. The analysis is divided into the individual efficiency of each part (battery, battery converter, EDLC pack, EDLC converter), but is also shown as the total efficiency and power loss of the whole system.

As the self-discharge of the EDLC pack is not strictly a power

loss issue but an energy loss issue, the units for measuring the loss are expressed as KJ.

Fig. 23 shows the difference between the FDAM, ADAM and the ATBM energy loss. The FDAM´s power loss is higher than the other two methods across all parts as well as the total energy loss. This is due to the aforementioned circulating currents between the battery and EDLC pack, caused by the delay of the battery. Thus it can be concluded that the FDAM´s performance is inferior to the ADAM and ATBM.

The ATBM uses more the EDLC than the ADAM, thus there is a higher energy loss due to the conducting losses. However, the battery losses are higher when using the ADAM, thus the objective

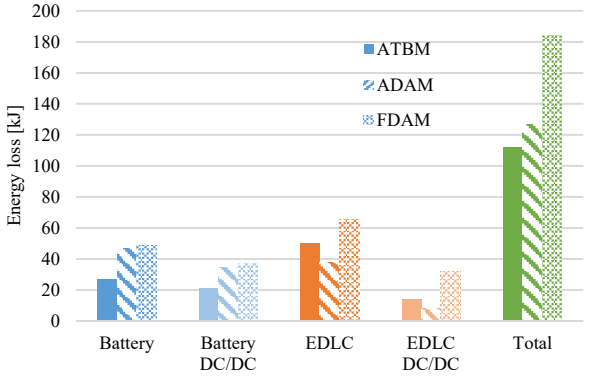

Fig. 23. Experimental ADAM and ATBM energy loss performance comparison.

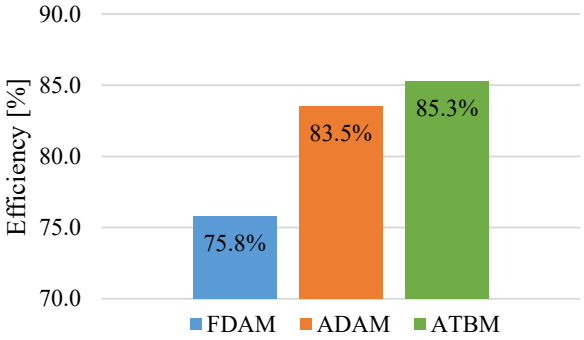

Fig. 24. Experimental ADAM and ATBM efficiency comparison.

of the proposed method, which was to lower the battery losses, is shown successful. When adding all the individual energy losses, it is clear that the proposed system is able to achieve a better energy performance, at about 12% loss reduction.

The efficiency data in Fig. 24 shows a similar outcome. The efficiency of the FDAM is 8% lower than the ADAM´s, while the ATBM is able to improve on the ADAM by 1.8%. This results show that the proposed method (ATBM) is higher performing than the two conventional methods (FDAM, ADAM) in terms of total system efficiency.

6. Conclusions

The paper proposes a high-efficiency control method for a grid fluctuation stabilization based on hybrid energy storage system. This method utilizes the characteristic differences of a battery pack and EDLC pack in order to determine the power reference of each, depending on the situation. The proposed method is applied in a 1 kW experimental setup, using a battery pack, EDLC pack and DC/DC converters. The proposed system is shown to be able to perform the energy balancing while having 1.8% higher efficiency than the conventional method. In addition, due to the nature of the method, the energy balance of the storage devices is controlled at all times. These results prove that the proposed method (ATBM) is better performing than the conventional methods (FDAM, ADAM).

References

(1) F. Blaabjerg, R. Teodorescu, M. Liserre, and A. V. Timbus : "Overview of Control and Grid Synchronization for Distributed Power Generation Systems", *IEEE Trans. On Industrial Electronics*, Vol.53, No.5, pp.1398-1409 (2006)

(2) E. Koutroulis and F. Blaabjerg, : "Design Optimization of Transformerless Grid-Connected PV Inverters Including Reliability", *IEEE Trans. On Power Electronics*, Vol.28, No.1, pp.325-335 (2013)

(3) J. V. Appen, Stetz, M. Braun, and A. Schmiegel : "Local Voltage Control Strategies for PV Storage Systems in Distribution Grids", *IEEE Trans. On Smart Grid*, Vol.5, No2, pp.1002-1009 (2014)

(4) P. M Carvalho, P. F. Correia, and L. A. Ferreira : "Distributed reactive power generation control for voltage rise mitigation in dist. Networks", *IEEE Trans. Power Syst.* Vol.23, pp.766-772 (2008)

(5) S. Suzuki, S. Maeshima, K. Morino, E. Shimoda, H. Sugihara, and T. Esaki. "Site Test in Micro-Grid into which a large amount of PV power generation system are introduced" *Te 2008 Annual Conference of Power and Energy Society, IEEJ,* no. 166, pp.11-12, 2008.

(6) H. Haga, T. Shimao, S. Kondo, K. Kato, Y. Itoh, K. Arimasu, K. Matsuda : "High-efficiency and cost-minimization method of energy storage system with multi storage devices for grid connection", *2014 International Power Electronics Conference (IPEC-Hiroshima 2014 - ECCE ASIA)*, pp.415-420 (2014)

(7) C. Zhao, H. Yin, Z. Yang, and C. Ma : "Equivalent Series Resistance-Based Energy Loss Analysis of a Battery Semiactive Hybrid Energy Storage System", *IEEE Trans. On energy Conversion*, Vol.30, No.3, pp.1081-1091 (2015)

(8) F. M. Gatta, A. Geri, S. Lauria, M. Maccioni, and F. Palone : "Battery storage efficiency calculation including auxiliary losses: Technology comparisons and operating strategies", *2015 IEEE Eindhoven PowerTech*, pp.1-6 (2015)

(9) T. Huria, M. Ceraolo, J. Gazzarri, R. Jackey : "High fidelity electrical model with termal dependence for characterization and simulation of high power lithium battery cells", *Vehicle Power and Propulsion Conference (VPPC)*, pp 1-6 (2015)

(10) M. Marracci, B. Tellini, o. Liebfried, and V. Brommer : "Experimental tests for Lithium batteries discharged by high power pulses", *2015* IEEE International Instrumentation and Measurement Technology Conference (I2MTC) Proceedings, pp.1063-1067 (2015)

(11) H. Nagasaki, P. Y. Huang and T. Shimizu, "Characterization of power capacitors under practical current condition using capacitor loss analyzer", *2016 IEEE Energy Conversion Congress and Exposition (ECCE)*, pp.1-7 (2016)

(12) P. Kulsangcharoen, C. Klumpner, M. Rashed and G. Asher, "A new duty cycle based efficiency estimation method for a supercapacitor stack under constant power operation", *5th IET International Conference on Power Electronics, Machines and Drives (PEMD 2010)*, pp.1-6 (2010)

(13) J. Kowal, E. Avaroglu, F. Chamekh, A. Senfelds, T. Thien, D. Wijaya, D. Uwe Sawer : "Detailed analysis of the self-discharge of supercapacitors", *Journal of Power Sources*, Vol.196, No.1, pp.573-579 (2011)

(14) Y. Diab, P. Venet, H. Gualous and G. Rojat : "Self-Discharge Characterization and Modeling of Electrochemical Capacitor Used for Power Electronics Applications", *IEEE Transactions on Power Electronics,* Vol.24, No.2, pp.510-517 (2009)

Elosegui Garcia Pablo (Non-member) received the B.E. degrees in energy and environmental science from Mondragon University, Hernani, Spain, in 2016. He is currently studying the master´s course in Electric, Electronic and Information Engineering at the Nagaoka University of Technology, Nagaoka, Japan. His research interests include power electronics.

Hitoshi Haga (Member) received the B.E., M.E. and D. Eng. degrees in energy and environmental science from the Nagaoka University of Technology, Nagaoka, Japan, in 1999, 2001, and 2004, respectively. From 2004 to 2007, he was a Researcher with Daikin Industries, Ltd., Osaka, Japan. From 2007 to 2010, he was an Assistant Professor with The Sendai National College of Technology, Sendai, Japan. Since 2010, he has been with the Nagaoka University of Technology, where he became an Associate Professor in 2016. His research interests include power electronics.